ENGINEERING TRANSACTIONS • *Engng. Trans.* • **51**, 4, 381–398, 2003
Polish Academy of Sciences • Institute of Fundamental Technological Research
10.24423/engtrans.478.2003

NUMERICAL MODELING OF LABORATORY TEST OF PLAIN CONCRETE UNDER UNIAXIAL IMPACT COMPRESSION

R. Adamczyk[(1)], T. Łodygowski[(2)]

[(1)]**Division of Theory of Structures, Technical University of Koszalin**
ul. Racławicka 15-17, 75-620 Koszalin

[(2)]**Institute of Structural Engineering, Poznań University of Technology**
ul. Piotrowo 5, 60-965 Poznań

The aim of this study is to compare experimental results of the behavior of concrete specimen, dynamically loaded in compression, carried out by P. H. BISCHOFF and S. H. PERRY [8], with the results obtained in numerical simulation. The intention of the investigation, reported in this paper, is to create the constitutive relation for concrete that depends on impact rates. The specimen was loaded in static as well as in dynamic tests. New constitutive relation of concrete dependent on impact rate has been proposed. Accuracy of the model was studied and compared with the experiment in simple $\sigma - \varepsilon$ characteristics. Two cases of concrete strength 30 and 50 MPa and three initial impact rates were considered. After verification in a simple uniaxial test, the new constitutive relation has been applied in complex engineering problem. Numerical impact analysis was carried out for impact tests in the environment of the ABAQUS/Explicit finite element code, and ABAQUS/Standard for static tests [1].

1. INTRODUCTION

Very often the engineers meet the problem how to estimate the behavior of a real structure in case of high strain rates [6]. The problem seems to be very complex, while there is no possibility of carrying out any experimental research due to economic reasons or impossibility of measuring the required values. In these cases the engineering design could be strongly supported by computer simulation [10].

The dynamic behavior of concrete depends on the strain rate [18]. While the strain rate increases, the parameters such as compressive strength of the concrete increases too, what may indicate a strength growth in terms of higher

strain rates, but corresponding to the stress values the strain increase as well, so the damage depends on plastic strain [4].

Among other problems to be solved such like building discrete model of such simulation, the fundamental importance has been focused on constitutive modeling [12]. Due to highly nonlinear, rate-dependent behavior of plain concrete, adoption of any model in the analysis is relatively complex and its application to finite element computer code is difficult [1]. Some comments and considerations concerning various aspects of numerical simulations of such phenomena were presented by CICHOCKI *et al.* [9]. To investigate complex engineering concrete structures under impact loading it is necessary to formulate proper constitutive model of the material [5]. This model should depend on the strain rates and include the failure criteria [3]. The only way to verify the constitutive relations, in case when we cannot carry out any experimental research, is to examine this material model in simple tests. These tests can also serve for calibration of the constitutive parameters.

In this paper, a new rate-dependent elastic-plastic (including tensile failure criterion) constitutive model for concrete was proposed. The basis for estimating rate-dependent characteristics for concrete were static characteristics given in paper [8] and experimental equations given in [19]. The rate-dependence was taken into consideration as an increase of strength, elastic modulus and strain dependent on the strain rate. This model was used to investigate the response of plain concrete in uniaxial compression test carried out by BISCHOFF and PERRY [8].

Results for two different concrete classes: 30 MPa and 50 MPa and three rates of strain: 9 s^{-1}, 5.2 s^{-1} and 5.6 s^{-1} of experiment [8] and numerical simulation were compared. The results of static test were also compared.

2. EXPERIMENTAL MOTIVATION

The laboratory tests of impact compression of the concrete specimens carried out by P. H. BISCHOFF and S. H. PERRY [8] were the experimental motivation for our study. The experiment was interesting because the authors reported the measured strain rates in specimens, velocity of the impacting mass, gave the characteristics $\sigma - \varepsilon$, and other values that are possible to calculate in numerical simulation. The report was a valuable basis for comparisons. The dimensions for concrete cylinders were 101.6 mm of diameter and 254 mm of height. The authors [8] used two mixes of concrete: 30 MPa and 50 MPa. In impact tests the specimens were loaded up to failure in the drop hammer machine shown schematically in Fig. 1, [16]. The 31.6 kg mass was dropped in impact tests at velocities 8–8.35 m/s and the 78.3 kg mass was dropped at velocities of 5–5.5 m/s. The deformation of concrete specimens was measured with strain gauges

located in the middle of their height on the surface. Axial compressive stress was measured at the base of the concrete specimens using a thin pressure load cell designed to minimize the errors caused by stress-wave reflection. For details see papers [8, 16].

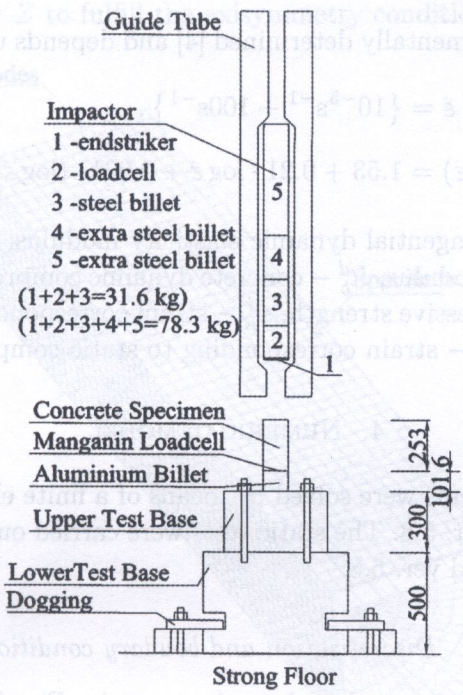

FIG. 1. Schematic view of impact test setup [8].

3. EXPERIMENTAL ACHIEVEMENTS

In dynamic strain response of concrete the values of elasticity modulus E_b^d increases due to static elasticity modulus E_b^{st}. Strains corresponding to dynamic strength ε_R^d also change due to static strains $\varepsilon_R^{\mathrm{st}}$. Experimental results [12] show that these values increase as the level of strain rate increases. The changes can be described by the following experimental equations (3.1) and (3.2) [19]:

$$\frac{E_{bt}^d}{E_{bt}^{\mathrm{st}}} = 1.061 + 0.0464 \cdot \log(\dot{\varepsilon}) + 0.00683 \cdot (\log \dot{\varepsilon})^2, \tag{3.1}$$

$$\frac{\varepsilon_R^d}{\varepsilon_R^{\mathrm{st}}} = 1.08 + 0.112 \cdot \log(\dot{\varepsilon}) + 0.0193 \cdot (\log \dot{\varepsilon})^2. \tag{3.2}$$

The factor of dynamic strength increase taken into consideration in this analysis is described by:

$$k_d = \frac{R_b^d}{R_b^{\mathrm{st}}}. \tag{3.3}$$

The factor was experimentally determined [4] and depends upon the strain rates:

$$\dot{\varepsilon} = \left\{10^{-5}\mathrm{s}^{-1} \div 100\mathrm{s}^{-1}\right\}, \tag{3.4}$$

$$k_d(\dot{\varepsilon}) = 1.53 + 0.21 \cdot \log \dot{\varepsilon} + 0.021 \cdot (\log \dot{\varepsilon})^2, \tag{3.5}$$

where E_{bt}^d – initial tangential dynamic elasticity modulus, E_{bt}^{st} – initial tangential static elasticity modulus, R_b^d – concrete dynamic compressive strength, R_b^{st} – concrete static compressive strength, ε_R^d – strain corresponding to dynamic compressive strength, $\varepsilon_R^{\mathrm{st}}$ – strain corresponding to static compressive strength.

4. Numerical model

The impact problems were solved by means of a finite element method using ABAQUS/Explicit ver. 5.8. The static tests were carried out in the environment of ABAQUS/Standard ver. 5.8.

4.1. Discretisation and boudary conditions

The problem was assumed to be axisymmetric, Fig. 2. Four nodes, bilinear axisymmetric, quadrilateral elements with reduced integration and hourglass control (CAX4R [1]) were used to define the geometry of the specimen. The analysis of the influence of mesh refinement on the results was carried out [7]. We considered five different cases: mesh 9×20 (180 elements), 9×50 (450 elements), 15×50 (750 elements), 15×100 (1500 elements) and 29×100 (2900 elements). We compared the results for different refinement for values such as strain rate, displacement of the specimen and stress in the specimen. The results confirmed the expected convergences so that the influence of space discretization was reasonably restricted. The time of computation was satisfactorily short for the mesh 15×50 elements (about 3–8 minutes, up to case). After discussion about the costs of computation and the demanded convergence accuracy, the mesh 15×50 (750 elements) was chosen and accepted to further analysis. The authors of the lab tests [8] didn't publish all the necessary details (base plate) to reproduce this experiment in numerical simulation. The point of the whole base with all its elements in the lab test was to create suitable boundary conditions (fixing) to eliminate the wave reflection influence and to be undeformable; that is why it is

so complex, large and massive. The simulation shows that we can not eliminate this phenomenon, so we have assumed ideal full fixing. We didn't consider the influence of full fixing of the specimen on the results in numerical simulation. To avoid any accidental errors of the influence of the base for results, we have decided to do such a simplification. Additional constraints had to be used on the axis the of symmetry Z to fulfill the axisymmetry conditions.

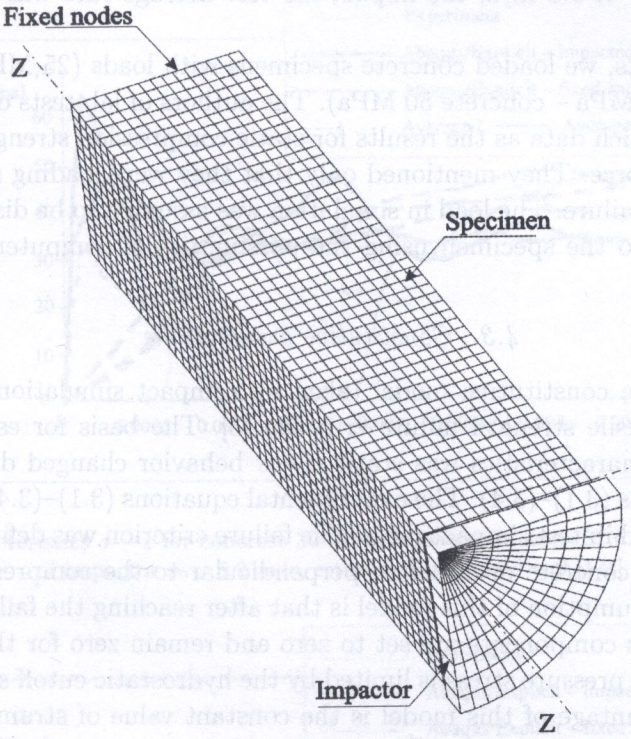

FIG. 2. Schematic view of modeled mesh (axisymmetric angle = 90°) .

4.2. Characteristics of impact and static loading

Concrete specimen was subject to dynamic loads by an element called "impactor". Impactor is the element that has much greater stiffness than concrete specimen (to avoid the influence of impactor material on the results) and has the same dimensions in all simulations. It was defined using the same type of finite elements as for the specimen. The change of mass of the impactor was assumed as a change of its density. The impact load was defined as an initial condition – velocity imposed on all nodes of the impactor. Gravity was also added. We assumed a contact between the specimen and impactor. The contact

was implemented between slave nodes of a specimen and master surface of the impactor. Between the specimen and impactor we created a gap of 1 mm to observe the close-up phenomenon. Mass of 31.6 kg was dropped on the specimen of concrete 30 MPa and concrete 50 MPa at the average lab tests velocities of 8.2 m/s and 5.3 m/s, the impact lab test average rates were estimated at 9.0 s^{-1} and 5.2 s^{-1}. The mass of 78.3 kg was dropped on concrete 50 MPa at the average velocity of 5.3 m/s, the impact lab test average rate was estimated at 5.6 s^{-1}.

In static tests, we loaded concrete specimens with loads (25 MPa – concrete 30 MPa and 45 MPa – concrete 50 MPa). The authors of lab tests didn't present in their paper such data as the results for static compression strength and value of destructive force. They mentioned only that they were loading statically the specimen until failure. The load in simulation was assumed to be distributed and put straight into the specimen using the possibilities of computer code procedure [1].

4.3. Constitutive assumptions

The concrete constitutive model taken into impact simulation was elastic-plastic with tensile strength failure criterion [3]. The basis for estimating the elastic-plastic characteristics was static $\sigma - \varepsilon$ behavior changed due to experimental equations (3.1)–(3.4). The experimental equations (3.1)–(3.4) were solved for the estimated in tests impact rates. The failure criterion was defined as tensile strength of the concrete in direction perpendicular to the compressive load direction. The assumption of this model is that after reaching the failure criterion, deviatoric stress components are set to zero and remain zero for the rest of the calculation, and pressure stress is limited by the hydrostatic cutoff stress [1]. The greatest disadvantage of this model is the constant value of strain rate in simulation. It has been proved that the strain rate is a strongly local phenomenon and is not constant in the whole element tested [14]. The constitutive model for concrete will be improved when the computational possibilities increase. In static simulation no failure criteria were applied.

5. Results of computations

The first values taken for comparison into consideration were characteristics $\sigma - \varepsilon$ for impact the tests. Figures 3, 4 and 5 show the characteristics $\sigma - \varepsilon$ for numerical tests compared with the lab experiment obtained by Bischoff and Perry [8]. The value of stress was determined as the sum of reaction forces in nodes of the cross-section divided by specimen area. The strain was determined as a sum of the displacement of the nodes on the top of the specimen divided by its initial length. The values of stress for the characteristics were taken in two

cross-sections: on the top, where impactor hits the specimen and on the base of the specimen. Solid line (thick) in Figs. 3, 4 and 5 shows the characteristics for $\sigma - \varepsilon$ at the impacted end. Thin solid line shows characteristics for $\sigma - \varepsilon$ at the fixed end. The dashed thick lines reflect the results of laboratory test. Two average curves: average I and average II were put on the diagram to close up to

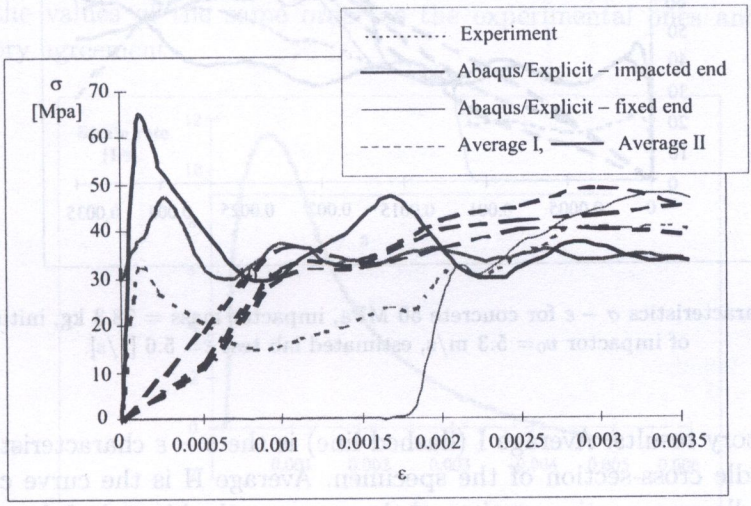

FIG. 3. Characteristics $\sigma - \varepsilon$ for concrete 30 MPa, impactor mass = 31.6 kg, initial velocity of impactor v_0= 8.2 m/s, estimated lab test $\dot{\varepsilon} = 9$ [1/s].

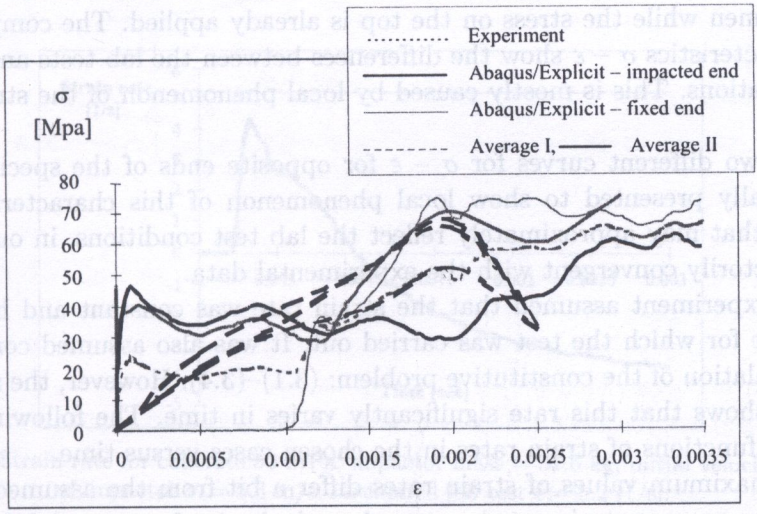

FIG. 4. Characteristics $\sigma - \varepsilon$ for concrete 50 MPa, impactor mass = 31.6 kg, initial velocity of impactor v_0= 5.3 m/s estimated lab test $\dot{\varepsilon} = 5.2$ [1/s].

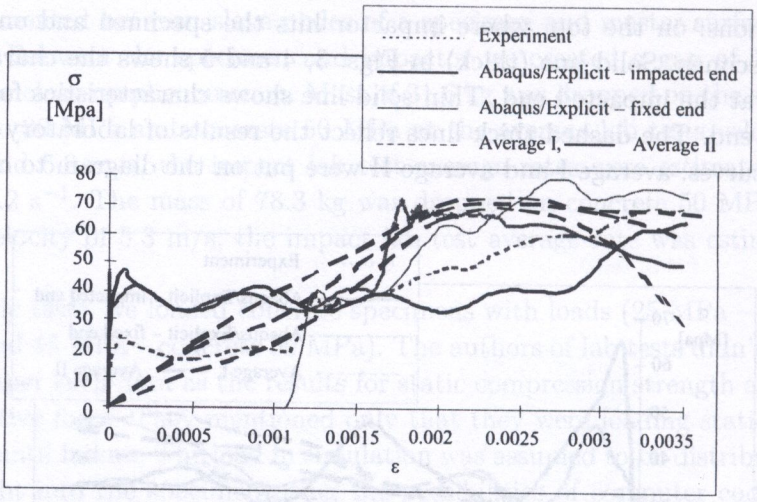

FIG. 5. Characteristics $\sigma - \varepsilon$ for concrete 50 MPa, impactor mass = 78.3 kg, initial velocity of impactor v_0= 5.3 m/s, estimated lab test $\dot{\varepsilon}$= 5.6 [1/s].

the laboratory results. Average I (dashed line) is the $\sigma - \varepsilon$ characteristics taken in the middle cross-section of the specimen. Average II is the curve computed due to middle cross-section strain and the stress on the hit end of the specimen. Average II gives the closest measurement conditions that were applied in laboratory tests. The curve average II does not start from the zero point like in the lab tests. The difference is the result of the delay of the strain in the middle of the specimen while the stress on the top is already applied. The comparison of the characteristics $\sigma - \varepsilon$ show the differences between the lab tests and numerical simulations. This is mostly caused by local phenomenon of the stress-strain values.

The two different curves for $\sigma - \varepsilon$ for opposite ends of the specimen were intentionally presented to show local phenomenon of this characteristic. The average, that may approximately reflect the lab test conditions, in our opinion is satisfactorily convergent with the experimental data.

The experiment assumed that the strain rate was constant and had a certain value for which the test was carried out. It was also assumed constant for the formulation of the constitutive problem: (3.1)–(3.4). However, the numerical analysis shows that this rate significantly varies in time. The following figures show the functions of strain rates in the chosen cases versus time.

The maximum values of strain rates differ a bit from the assumed ones. In lab test the average strain rate is counted on the basis of measured deformations in time due to strain gauge placed in the middle of the specimen height on its surface. In simulation, an average as a sum of the nodes displacement in the whole

cross-section in the middle of specimen was considered as a function of time. These rates taken in different cross-sections of the specimen show differences, generally the diagram has the same shape but the values differ. This may point on the strongly local phenomenon of strain rate [17], what contradicts statement found in paper [8] about the level of average strain rate.

We consider that in spite of differences in assumptions our constitutive model reaches the values of the same order as the experimental ones and gives us satisfactory agreement.

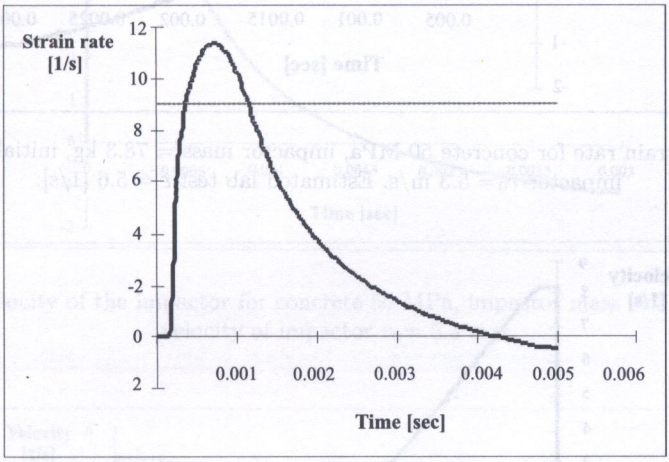

FIG. 6. Strain rate for concrete 30 MPa, impactor mass = 31.6 kg, initial velocity of impactor v_0= 8.2 m/s. Estimated lab test $\dot{\varepsilon} = 9$ [1/s].

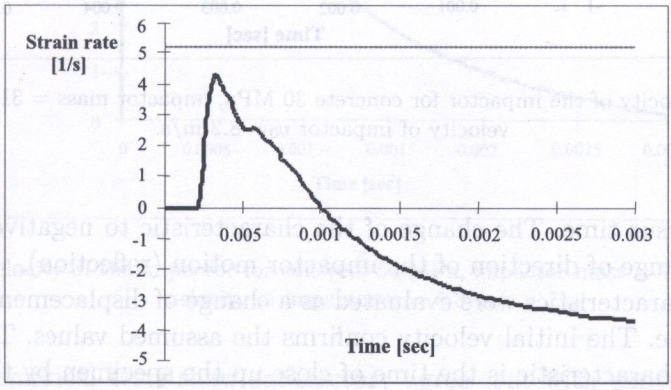

FIG. 7. Strain rate for concrete 50 MPa, impactor mass = 31.6 kg, initial velocity of impactor v_0= 5.3 m/s. Estimated lab test $\dot{\varepsilon} = 5.2$ [1/s].

The change of velocity of impactor is shown in the following figures (Figs. 9, 10 and 11). This value was determined due to velocity of the contact nodes of the

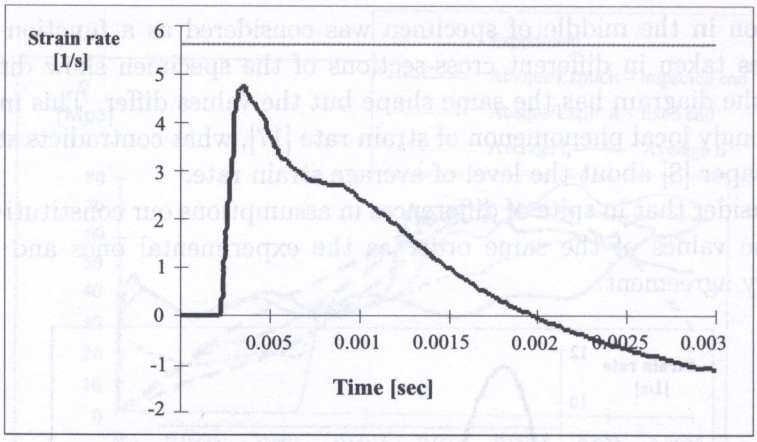

FIG. 8. Strain rate for concrete 50 MPa, impactor mass = 78.3 kg, initial velocity of impactor v_0= 5.3 m/s. Estimated lab test $\dot{\varepsilon} = 5.6$ [1/s].

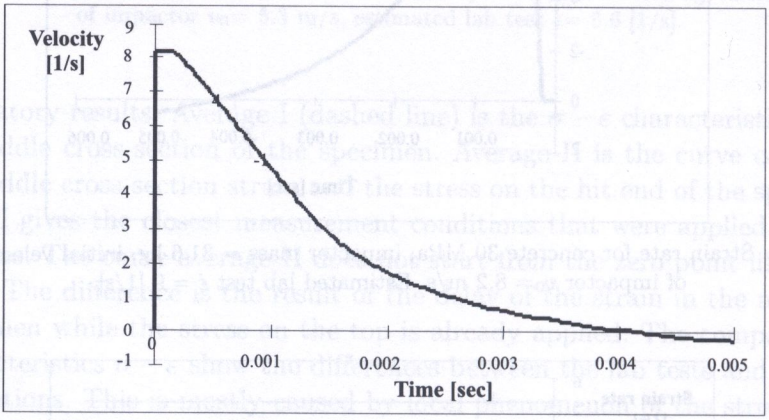

FIG. 9. Velocity of the impactor for concrete 30 MPa, impactor mass = 31.6 kg, initial velocity of impactor v_0= 8.2 m/s.

impactor versus time. The change of the characteristic to negative values indicates the change of direction of the impactor motion (reflection).

These characteristics were evaluated as a change of displacement of impactor nodes in time. The initial velocity confirms the assumed values. Time of linear part of the characteristic is the time of close-up the specimen by the impactor.

When comparing the two first figures (Fig. 9 and Fig. 10) we see the same dropping mass on concrete with different compression strength. Comparison of Fig. 10 and Fig. 11 shows the results for the same compression strength of concrete and different dropping masses. The point of rebound is a point where the curve is reaching zero. When the curve is below zero, the impactor is going up

after rebounding. We can find that in case when the strength of the concrete is greater (larger density and Young modulus), the same dropping mass is rebounding in a shorter time. When the dropping mass is greater, in case of the same compression concrete strength, the impactor is rebounding in a longer time.

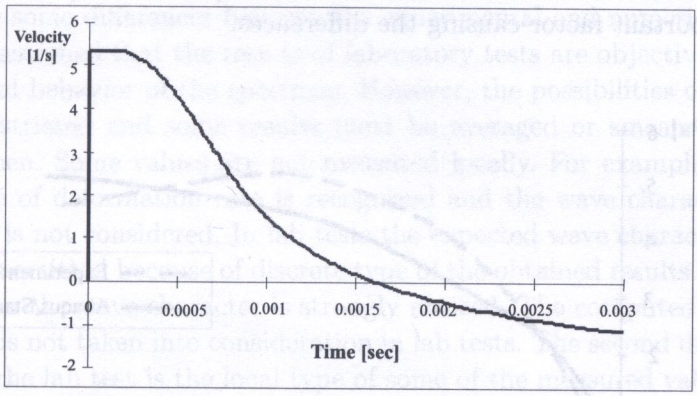

FIG. 10. Velocity of the impactor for concrete 50 MPa, impactor mass = 31.6 kg, initial velocity of impactor v_0= 5.3 m/s.

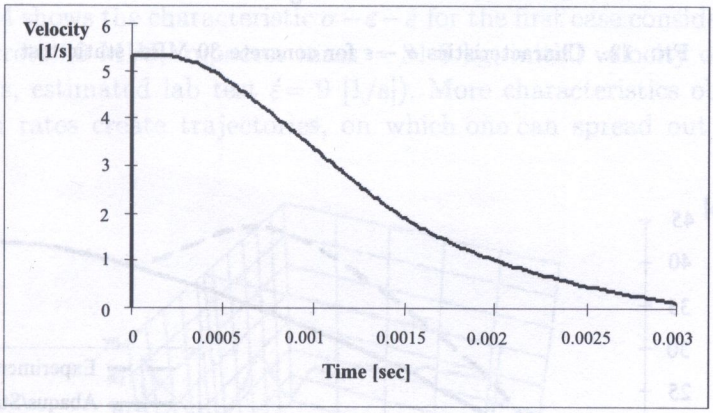

FIG. 11. Velocity of the impactor for concrete 50 MPa, impactor mass = 78.3 kg, initial velocity of impactor v_0= 5.3 m/s.

Static numerical tests show satisfactory agreement with experimental tests but the differences can be still noticed in Figs. 12, 13. The stress in the characteristic was obtained as a reaction force at the fixed end of the specimen converted to its cross-section, and strain was computed as an average displacement of nodes on the loaded surface converted to specimen length. The differences in characteristics may be caused by discrete and surface-like experimental test. The strain

gauges in experimental tests were put on the surface of the specimen and values were taken in a discrete way, while in numerical test the average value in cross-section was considered in a continuous way. In spite of these differences the maximum values of stresses are similar in both cases. Numerical static tests consider constitutive concrete models without any failure criterion; this may be also an important factor causing the differences.

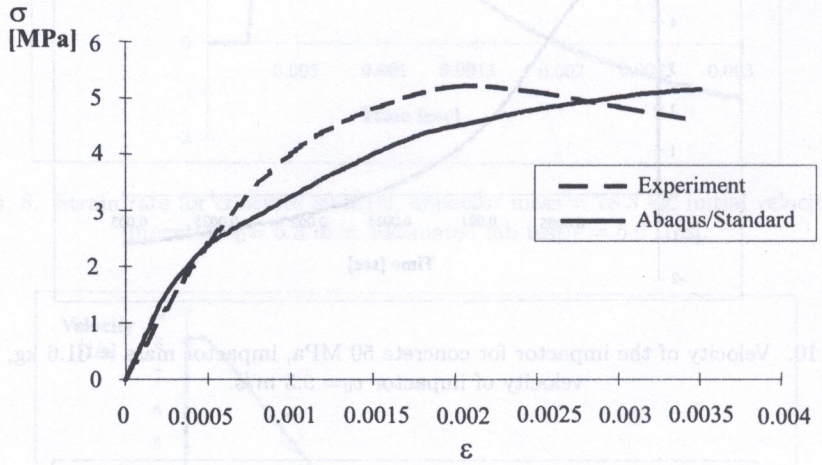

FIG. 12. Characteristics $\sigma - \varepsilon$ for concrete 30 MPa, static test.

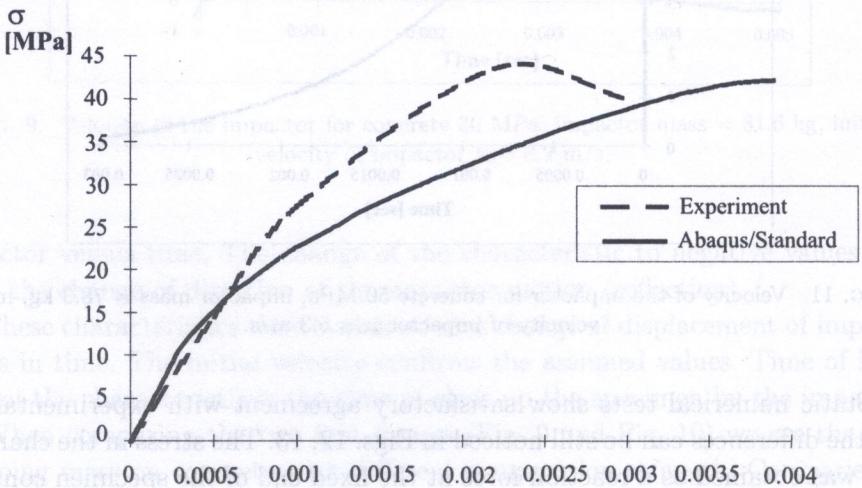

FIG. 13. Characteristics $\sigma - \varepsilon$ for concrete 50 MPa, static test.

6. Conclusions

Concrete is one of the engineering materials which, when subjected to high rates of loading usually associated with impacts, shows increase of the value of elastic modulus, compressive strength and the values associated with them.

There are some differences between the experimental and numerical results. It should be assumed that the results of laboratory tests are objective and they reflect the real behavior of the specimen. However, the possibilities of measurements are restricted and some results must be averaged or smeared over the whole specimen. Some values are not measured locally. For example, only the average value of deformation rate is recognized and the wave character of the phenomenon is not considered. In lab tests the expected wave character of phenomenon was omitted because of discrete type of the obtained results. In numerical simulation the wave character is strongly noticed. The computed values are varied, what is not taken into consideration in lab tests. The second drawback of interpreting the lab test is the local type of some of the measured values, which are considered as average. In the experiment the main value the strain rate, was treated as a constant and average in the whole specimen. Numerical simulation shows that it is variable in time and has a local character, and when it is taken from different cross-sections in the specimen, it shows completely different values.

Figure 14 shows the characteristic $\sigma - \varepsilon - \dot{\varepsilon}$ for the first case considered in this paper (concrete 30 MPa, impactor mass = 31.6 kg, initial velocity of impactor v_0= 8.2 m/s, estimated lab test $\dot{\varepsilon}$= 9 [1/s]). More characteristics obtained for other strain rates create trajectories, on which one can spread out a surface.

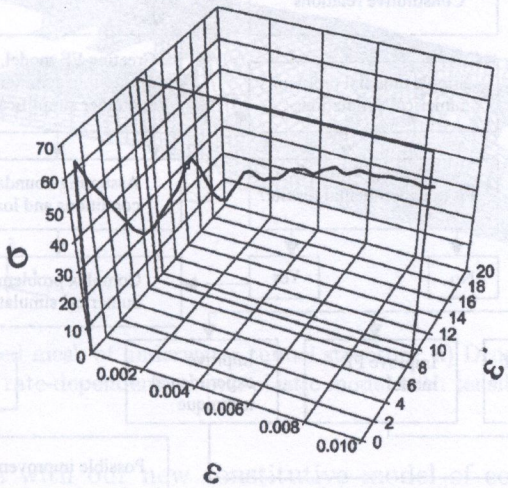

FIG. 14. Characteristic $\sigma - \varepsilon - \dot{\varepsilon}$ for concrete 30 MPa, impactor mass = 31.6 kg, initial velocity of impactor v_0= 8.2 m/s, estimated lab test $\dot{\varepsilon}$= 9 [1/s].

This surface can be a base for the solution for the used concrete constitutive model. A plane for constant value of strain rate 9 [1/s] is added to show the strain rate estimated in lab test and its intersection with non-constant diagram of strain rate obtained in numerical simulation.

In spite of differences between the lab and numerical tests we may consider this material constitutive model for concrete to be verified and valid in impact tests in this range of strain rates. The box scheme in Fig. 15 shows the proposal of the method for verification of such constitutive material models. The constitutive model calibrated in this way may be used to solve more complex engineering problems that can not be tested in the lab conditions.

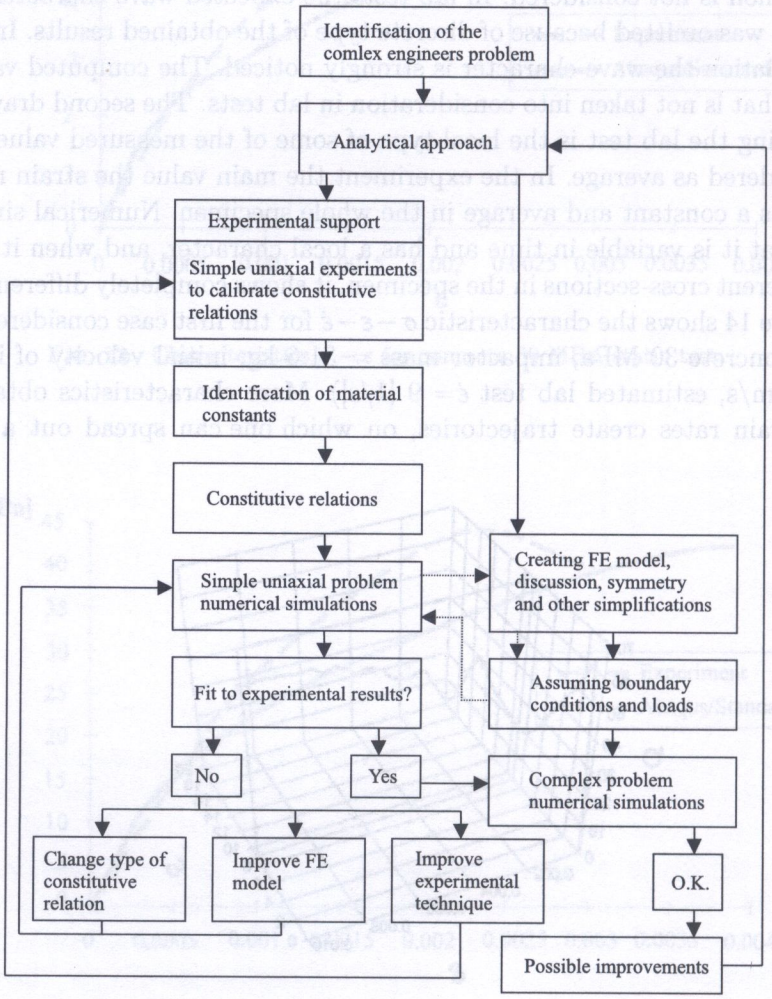

FIG. 15. The solution procedure of the complex engineering analysis in box scheme.

The new constitutive material model we have applied in a very complex engineering structure. This structure is an underwater tunnel loaded by explosion of 40 kg of spherical charge of trinitrotoluene (described in details in [11]). The description of pressure was obtained on the basis of semi-empirical equations proposed by HENRYCH [15]. For the reasons of scale and kind of load, this structure doesn't have any laboratory tests of behavior. We considered two material models for concrete. First: the Drucker–Prager model [1, 13], available in ABAQUS code, and second: our rate-dependent, elastic-plastic model with tensile failure criteria verified by uniaxial laboratory test. The results of comparison are shown in Fig. 16 and Fig. 17. In Fig. 16 the deformed meshes of structure for constitutive models are presented and Fig. 17 shows equivalent plastic strain in a concrete layer of sandwich, the main structural layer of the tunnel.

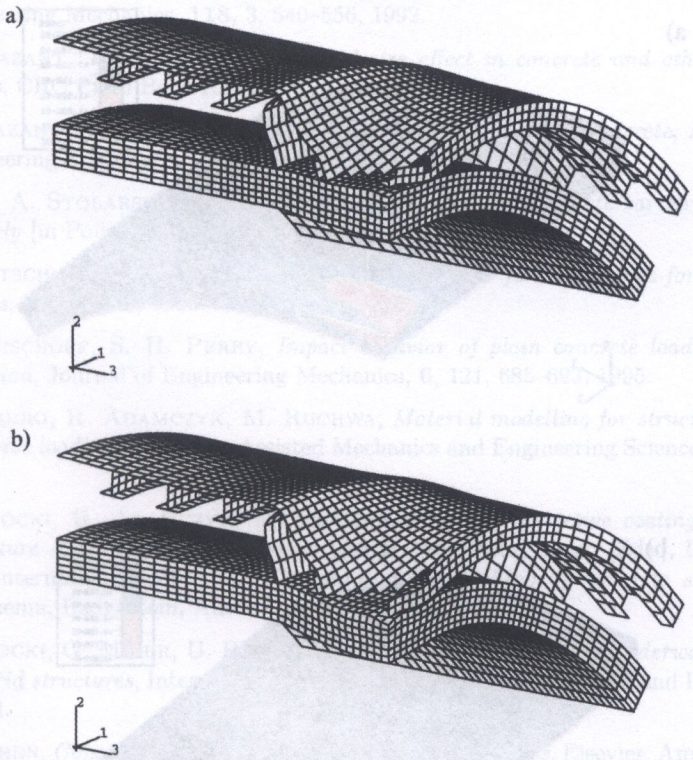

FIG. 16. Deformed mesh of underwater tunnel structure: a) Drucker–Prager model for concrete, b) rate-dependent, elastic-plastic model with tensile failure criteria.

In the version with our new constitutive model of concrete, the structure reveals greater increase of concrete core deformation. It means that in this case, the area of destruction in concrete is larger than in the case with constitutive

model of Drucker–Prager. This presumption is confirmed in Fig. 17, which shows equivalent plastic strain in concrete layer of a sandwich. One can conclude that if we don't consider the strain rate in our constitutive model for impacted loaded concrete, we can overestimate the ultimate load capacity of the structure what is dangerous for the design.

Laboratory tests should be strongly supported by numerical analysis to avoid mistakes in interpreting the results. There is a need to carry out the numerical analysis before the laboratory tests are prepared to estimate the details of response of the structure or material and to support and create the proper project of laboratory tests. The numerical model for concrete used in this test will be improved and adapted to the variable in time strain rates.

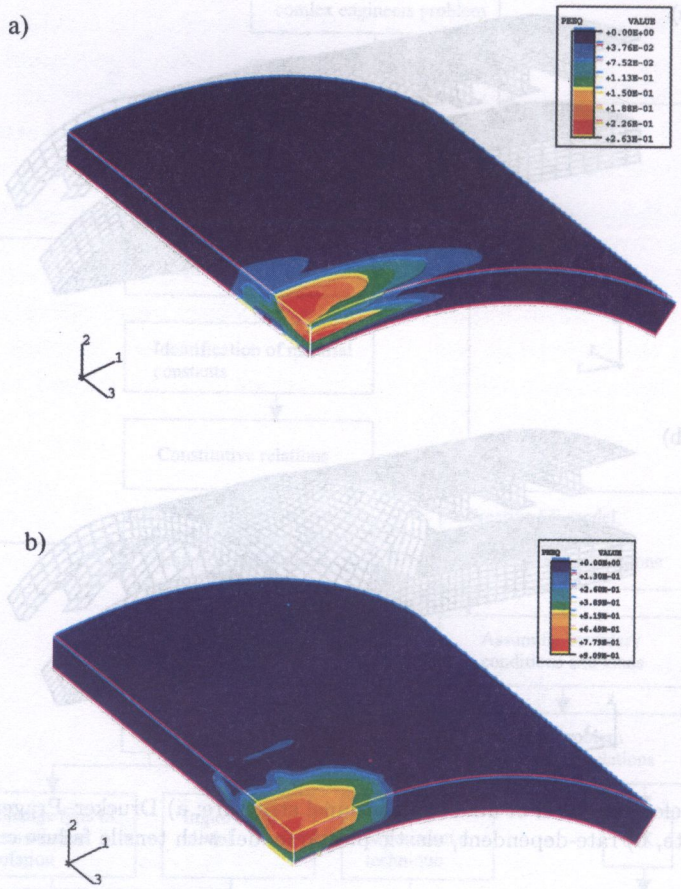

FIG. 17. The contour plot of equivalent plastic strain in concrete layer of the sandwich: a) Drucker–Prager model for concrete, b) our rate-dependent, elastic-plastic model with tensile failure criteria.

ACKNOWLEDGMENT

The support of the Poznań University of Technology grant BW-11-167/02 was very helpful. Some of the computations were performed in the Poznań Supercomputing and Networking Centre.

REFERENCES

1. ABAQUS 5.8 *Manuals*, Hibbit, Karlson & Sorensen Inc., 1999.
2. Z. P. BAZANT, *Modelling of compressive strain softening, fracture and size effect in concrete*, [in:] R. DE BORST *et al.* [Eds.], Proceedings of Euro-C International Conference *Computational Modelling of Concrete Structure*, 623–631, Balkema, Badgastein, Austria.
3. Z. P. BAZANT, J. OZBOLT, *Compression failure of quasibrittle material*, ASCE Journal of Engineering Mechanics, **118**, 3, 540–556, 1992.
4. Z. P. BAZANT, J. PLANAS, *Fracture and size effect in concrete and other quasibrittle materials*, CRC Press Boca Raton and London, 1998.
5. Z. P. BAZANT, Y. XIANG, P. C. PRAT, *Microplane model for concrete*, ASCE Journal of Engineering Mechanics, **122**, 3, 245–254, 1996.
6. G. BĄK, A. STOLARSKI, *Nonlinear analysis of reinforcde concrete bar structures loaded impulsively* [in Polish], PAN, Warszawa 1990.
7. T. BELYTSCHKO, W. KAM LIU, B. MORAN, *Nonlinear finite elements for continua and structures*, Wiley Ltd., 1999.
8. P. H. BISCHOFF, S. H. PERRY, *Impact behavior of plain concrete loaded in uniaxial compression*, Journal of Engineering Mechanics, **6**, 121, 685–693, 1995.
9. K. CICHOCKI, R. ADAMCZYK, M. RUCHWA, *Material modelling for structures subjected to impulsive loading*, Computer Assisted Mechanics and Engineering Sciences, **6**, 231–244, 1999.
10. K. CICHOCKI, R. ADAMCZYK, M. RUCHWA, *Effect of protective coating on underwater structure subjected to an explosion* [in:] R. DE BORST *et al.* [Eds.], Proceedings of Euro-C International Conference *Computational modelling of concrete structure*, 623–631, Balkema, Badgastein, Austria 1998.
11. K. CICHOCKI, G. MAIER, U. PEREGO, *Analysis of damages due to underwater explosions on a hybrid structures*, International Journal for Engineering Analysis and Design, **1**, 341-361, 1994.
12. W. F. CHEN, *Constitutive equations for engineering materials*, Elsevier, Amsterdam 1994.
13. Y. C.FUNG, *Foundations of solid mechanics* [in Polish], PWN, Warszawa, 1969.
14. A. GLEMA, T. ŁODYGOWSKI, P. PERZYNA, *Interaction of deformation waves and localization phenomena in inelastic solids*, Computer Methods in Applied Mechanics and Engineering, 183, 123–140, 2000.
15. J. HENRYCH, *The dynamics of explosions and its use*, Elsevier, Amsterdam 1979.
16. S. H. PERRY, P. H. BISCHOFF, *Measurement of the compressive impact strength of concrete using a thin loadcell*, Mag. of Concrete Res., **42**, 151, 75–81, 1990.

17. P. PERZYNA, *Fundamental problems in viscoplasticity*, *Advances in applied mechanics*, Academic Press, New York, **9**, 244–368, 1966.

18. P. SOROUSHIAN, K. B. CHOI, A. ALHAMAD, *Dynamic constitutive behaviour of concrete*, J. ACI, **83**, 2, 251–259, 1986.

19. Z. SZCZEŚNIAK, *Modeling of the dynamic behaviour of underground structures under impact air wave*, WAT, Warszawa 1999.

Received December 15, 2002; revised version July 7, 2003.